AJOMC

Asian Journal of Organic & Medicinal Chemistry

http://ajomc.asianpubs.org

Editor-in-Chief

Dr. Bimal K. Bainik

Vice President of Research & Education Development
Community Health Systems of South Texas
Edinburg, USA

Principal
Jawahar Arts, Science & Commerce College,
Andur Tal. Tuljapur Dist, Osmanabad

Infra-red Spectroscopy and Elasticproperties of Ce³⁺ Ion Substituted Cu-Zn Ferrite

J. Patil[1,*], U. Chanshetti[2] and C. Pawar[2]

[1]Department of Chemistry, Dr. Babasaheb Ambedkar Marathwada University, Aurangabad, India
[2]Department of Chemistry, Kaviyatri Bahinabai Chaudhari North Maharashtra University, Jalgaon, India

ABSTRACT

$Cu_{0.5}Zn_{0.5}Ce_xFe_{2-x}O_4$ (x = 0.0, 0.025, 0.05, 0.075, 0.1) ferrite nanoparticles were synthesized by using the sol-gel auto-combustion approach.The synthesized samples were sintered at 600 degree for 4 hours. Infrared spectra have been completed at room temperature within the wavenumber variety of 300-800 cm⁻¹. The IR spectra display principal absorption bands. High-frequency bands 'v_1' is assigned to the tetrahedral and coffee-frequency bands 'v_2' are assigned to the octahedral sites of the complex. The Force consistent for the tetrahedral and octahedral sites changed is study by the usage of IR information. Force constant values is used to calculate the Stiffness constants (C_{11} and C_{12}). Considering the values of stiffness constants; Elastic moduli consisting of young's modulus, Rigidity modulus, Poisson's ratio, and Debye temperature are calculated.

KEYWORDS: Sol-gel method, Ferrites, Infra-red spectroscopy, Elastic property.

INTRODUCTION

Cu-Zn spinel ferrites have wide varietyof applicationslike non-resonant devices, radio frequency circuits, read/write heads for high-speed digital tapes, and microwave devices. [1-2] The small addition of external ions can change the ferrite identity along with their properties.[3] The spinel ferrites properties such as structural, magnetic, and electrical are basedon cation distribution of cations in between tetrahedral [A] and octahedral (B) site of spinel structure.[4]Infrared spectroscopy (IR).[5]Structural evaluationgives useful details about the spinel structure. The technique is based upon selective adsorption in the IR.The tetrahedral (A) and octahedral [B] sites of spinel ferrites show absorption bands in the IR spectra split based on cations distribution on them.[6–8]Study of elastic behaviours of ferrites providesthe informationof interatomic and interionic forces in them. Ferrites are very strong and cannot be deformed under normal conditions.[9-11] Ferrites samples were prepared in several methods. Such as Solid-state reaction[12]. Hydrothermal preparation[13], Micro emulsion method[14], Oxalate Precursors method [15]. Now a day, among these various preparation methods of the ferrite nanoparticles, like Sol-gel auto-combustion techniques[16]. The elastic constant is presents nature of the binding forces in the solid. The mechanical strength, fracture toughness and thermal resistance information study by elastic modulus [17]. Study of elastic properties is examined by the synthesis of $Cu_{0.5}Zn_{0.5}Ce_xFe_{2-x}O_4$ (x = 0.0, 0.025, 0.050, 0.075, 0.1) using Sol-gel Auto-Combustion method along with effect of Ce³⁺ substituted in prepare ferrites.

EXPERIMENTAL

Nanocrystalline ferrite powders with compositions of $Cu_{0.5}Zn_{0.5}Ce_xFe_{2-x}O_4$ (x = 0.0,0.025,0.05,0.075,0.1) were synthesized by Sol-gel Auto-Combustion technique. Shown in the fig.1. The metal nitrates (A.R. grade with 99.8 % purity) Copper Nitrate, $Cu NO_3)_26H_2O$, Zinc nitrate (Zn $(NO_3)_2.6H_2O$), ferric nitrate ($Fe(NO_3)_2.9H_2O$), Cerium nitrate ($Ce(NO_3)_36H_2O$), and citric acid ($C_6H_8O_7.H_2O$), were used as starting materials. The reaction was carried out in the air atmosphere without the protection of inert gases. The molar ratio of metal nitrates to citric acid was taken as 1:3. The metal nitrates were dissolved together in a minimum amount of double distilled water to get a clear solution. An aqueous solution of citric acid was mixed with metal nitrates solution, then ammonia solution was slowly added to adjust the pH ≅ 7. The mixed solution was kept on to a hot plate with continuous stirring at 90 °C. During evaporation, the solution became viscous and finally formed a viscous brown gel. When finally, all water molecules were removed from the mixture, viscous gel began frothing. After few minutes, the gel automatically ignited and burnt with glowing flints. The decomposition reaction would not stop before the whole citrate complex was consumed. The auto-combustion was completed within a minute, yielding the brown-colored ashes termed as a precursor. The as-prepared powder was then annealed at 600 °C for 4 hrs. The infrared spectra of all the samples were recorded at room temperature in the range 200 cm⁻¹ to 800 cm⁻¹.on Perkin Elmer infrared Spectrophotometer.

Sol-gel Auto-combustion

Metal nitrate and Citric acid

(1:3) ratio in Double distill water

↓

mixed above solution

↓

Clear solution of nitrates · citric acid

Ammonia is added till

↓

till pH ≈ 7

↓

Continuous stirring at 90° C

Evaporation

↓

Viscous brown gel formed

↓

Frothing

Ignite

↓

Burnt with glowing flints

Auto -combustion

↓

Brown colored ashes (precursor)
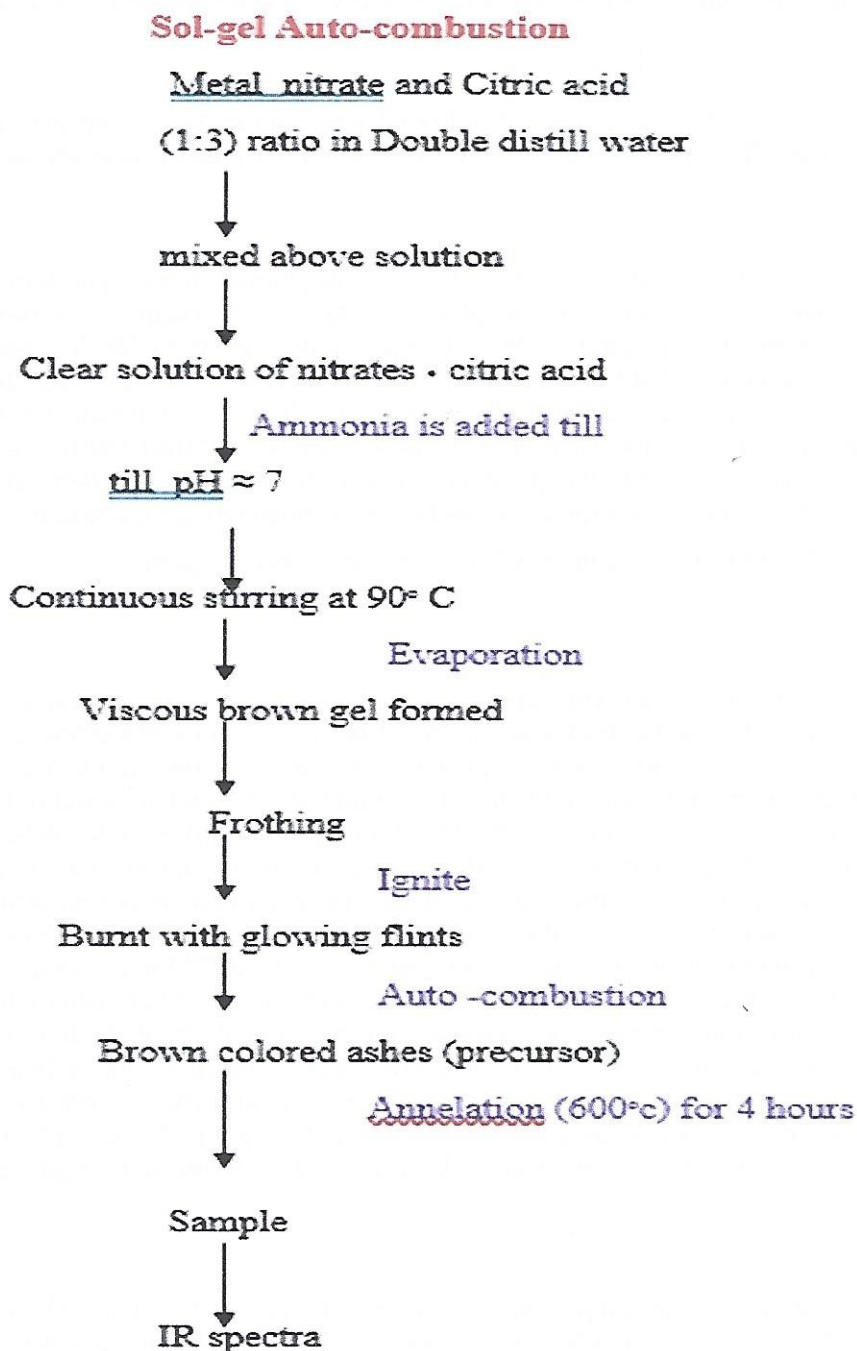
Annelation (600°c) for 4 hours

↓

Sample

↓

IR spectra

Fig.1.Schematic diagram for the Sol-gel auto-combustion method.

RESULTS AND DISCUSSION

Infra-Red Spectroscopy: NanocrystallineCu$_{0.5}$Zn$_{0.5}$Ce$_x$Fe$_{2-x}$O$_4$ ferrite system is illustrated in Fig. 2. IR spectrum in the range of 200-800 cm^{-1}. The investigated absorption band was listed in Table 1. It is observed from Table 1. IR spectrum displayed two absorption bands at562-627 and 362-418 cm^{-1} for the spinel ferrites. The better frequency band (v_1) become due to the stretching vibration of the tetrahedral metallic-oxygen bond and the decrease frequency band (v_2) changed into because of the octahedral steel-oxygen bond [13]. The band positions for all of the investigated compositions are given in Table 1. The trade inside the lattice constant is chargeable for this shift of the middle frequencies. The increase inside the unit mobile dimensions due to the substitute of Fe^{3+} ions via large ionic radius Ce^{3+}ions affect the Fe^{3+}- O^{2-}stretching vibrations and that is a distinguished reason of trade in band positions. The change inside the frequency of the v_1 stretching band suggests the choice of Ce^{3+}ions to occupy the octahedral web sites. The height intensity of frequency bands

slightly changes with growing Ce^{3+} substitution. It is understood that the depth ratio is a feature of the trade of dipole moment with the inter-nuclear distance (dμ/dr) [14]. This fee represents the contribution of the ionic bond Fe-O inside the lattice. Furthermore, it's miles determined from Fig. 2. that the regular mode of vibration of a tetrahedral cluster(v_1) is higher than that of the octahedral cluster(v_2), that is attributed to the shorter bond period of tetrahedral cluster and longer bond period of octahedral cluster. Using the analysis of Waldron [5], the force regular K0 and Kt were calculated.
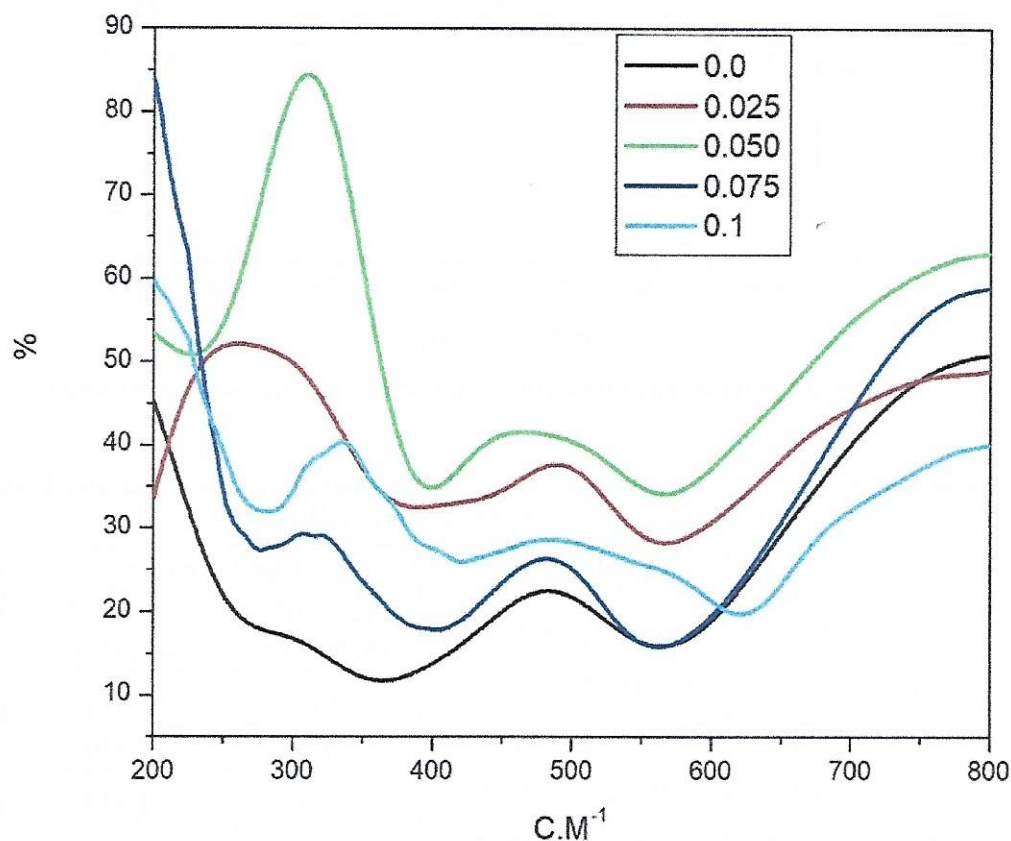

Fig 2. Infrared spectra for the series $Cu_{0.5}Zn_{0.5}Ce_xFe_{2-x}O_4$.

According to Waldron the force constant K_t and K_o for respective sites are given by:

$$K_t = 7.62 \times M_1 \times v_1^2 \times 10^{-3} \qquad (1)$$

$$K_0 = 10.62 \times \frac{M_2}{2} \times v_2^2 \times 10^{-3} \qquad (2)$$

Where, K0 = pressure regular on octahedral site, Kt = force regular on tetrahedral web site, M1=Molecular weight of tetrahedral web site, M2=Molecular weight of octahedral web page, v_1=Corresponding centre frequency on tetrahedral web page, v_2 = Corresponding middle frequency on octahedral website online. The values of forces are summarized in Table 1. The force constant Kt increasing with the increasing Ce^{3+} content whereas Ko will increase with the increase in Ce^{3+}. This variation can be associated with the distinction in ionic radii of Fe^{3+} and Ce^{3+} ions and their occupancy at A and B web sites. Analysis of IR spectra with crystallographic know-how enables us to decide the Debye temperature and elastic houses. The Debye temperature (θI) of all samples turned into calculated the usage of the wavenumber of IR bands.[14].

$$\theta l = hCVac/k \qquad (3)$$

Where, h = h/2π, ok is Boltzmann constant, C is the speed of mild (C = 3×10^8 cm/s) and V_{av} is the common wave quantity of bands. Variation of Debye temperature with Ce^{3+} content material is proven in Fig.3.
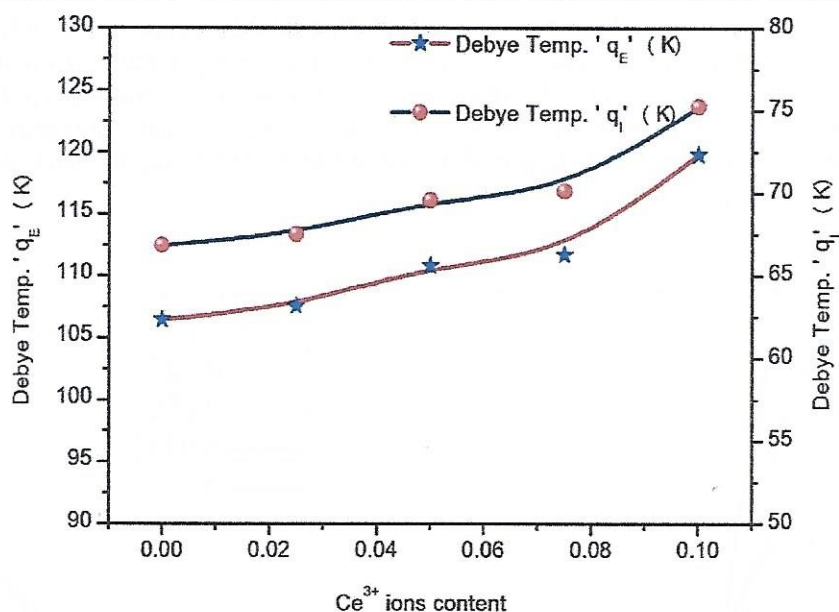
Fig.3. Variation of Debye temperature calculated from infrared (θl) and elastic (θ_E)data with Ce^{3+} content.

Table No.1: $Cu_{0.5}Zn_{0.5}Ce_xFe_{2-x}O_4$ of (a), (dx), (v_1 and v_2), (K_o and K_t) are Lattice constant, X-ray Density, Band Position, force constant respectively.

Comp. x	'a' (Å)	'd$_x$' (g/cm^3)	Band position		Force constant	
			v_1(cm^{-1})	v_2 (cm^{-1})	K_0 x 10^5 (dyne/cm)	K_t x 10^5 (dyne/cm)
0.0	8.364	5.353	566.41	362.45	0.814	1.404
0.025	8.373	5.369	570.63	367.92	0.838	1.429
0.05	8.394	5.371	571.3	395.51	0.968	1.439
0.075	8.415	5.386	575.17	399.64	0.988	1.467
0.1	8.421	5.391	627.14	418.34	1.079	1.745

Elastic Properties: The elastic properties had been decided the use of infrared spectroscopy [18-20] These elastic moduli have been calculated the usage of the values of lattice constant 'a', X-ray density 'dx', pore fraction 'f', and force constant 'K'. Values of lattice constant, X-ray density, and pore fraction are listed in Table 1. The average force steady (K) changed into calculated using the subsequent relation:

$$k = kt + ko/2 \qquad (4)$$

The bulk modulus of term stiffness constant C_{11} was calculated using relation [17] Stiffness constant is attributed to interatomic binding between metal ions like Fe, Ce, Zn and Co etc in the present ferrite system.

$$C_{11}. a = K \qquad (5)$$

Where, a and Kis the lattice constant andaverage force constant respectively

$$\text{Stiffness constant } (C_{12}) = \frac{\sigma \times C11}{(1-\sigma)} \qquad (6)$$

Where,σ and ais the Poisson ratio and lattice constant respectively. The $\sigma = 0.324 \times 1 - 1.043f$ is function of pore fraction of Poisson ratio. Table 2. represents the Poisson ratio ranges between 0.273 and 0.264, These values lie inside the range of -1 to 0.5, which conforms with the principle of isotropic elasticity. [13]. Variation of stiffness constants (C_{11} and C_{12}) as a characteristic of Ce3+content material is shown in table.2. It is discovered from Table .2. Both the stiffness steady elevated with a boom in Ce^{3+} substitution. The values of Poisson's ratio had been calculated using the relation mentioned somewhere else [17] and the values are offered in Table 2.

Special Issue on Current Research in Chemistry and Nanosciences (CRCNS-2022) Jawahar Arts, Science & Commerce College, Andur Tal. Tuljapur Dist, Osmanabad

106

Stiffness constant is tormented by elements. The tightness of bonding between the atoms and pressure steady. In the present machine bonds between Fe^{3+} and Ce^{3+} atoms are residual bonds and due to this stiffness constant increases with growing Ce^{3+} content material.

Table No.2: $Cu_{0.5}Zn_{0.5}Ce_xFe_{2-x}O_4$ of (K),Pore fraction, σ, (C_{11} and C_{12}) are Mean force constant, Passion's ratio, Stiffness constant respectively.

Comp. x	Mean Force constant (K) (K_t+K_o)	Pore Fraction	Passion's ratio σ	C_{11}	C_{12}
0.0	1.109	0.138	0.274	132.63	50.057
0.025	1.134	0.144	0.270	135.38	50.073
0.05	1.204	0.148	0.269	143.38	52.761
0.075	1.228	0.157	0.268	145.89	53.413
0.1	1.412	0.162	0.267	167.69	61.081

These 2 stiffness constants used to calculate elastic constants such as; Young's modulus (E), bulk modulus (K), and modulus of rigidity (G) [14]. The elastic moduli for cubic structure are calculated as follow [18.].

$$(G) = \frac{E}{2(\sigma+1)} \qquad (7)$$

The rigidity modulus (G) is calculated using relation 3 and the version is offered in Table 3. It may be found from Table.3. The values of rigidity modulus increased with Ce^{3+} substitution. B, G, E increases with a growth in both Ce^{3+}. It indicates that deformation of the solid is easy and the strong has less tendency to spring again to its equilibrium role. The Young's modulus, Bulk modulus, and modulus of rigidity boom with the increasing Ce^{3+} content. They will increase in elastic moduli may be because of the interatomic binding between diverse atoms in the spinel lattice.[20]. The inter-atomic bonding among the diverse atoms weakens continuously with the addition of Ce^{3+} content and consequently elastic moduli boom with the increasing Ce^{3+} content material. In $Fe^{3+} - Ce^{3+}$ ferrite repulsion among electrons can be multiplied with the increasing Ce3+content. [14].

The longitudinal elastic wave speed (VL) and transverse (Shear) wave pace (VS) became calculated the usage of the subsequent equations,

$$\text{Longitudinal velocity} \quad V_L = \left(\frac{C_{11}}{\rho}\right)^{1/2} \qquad (8)$$

$$\text{Transverse (Shear) velocity} \quad V_S = \left(\frac{G}{\rho}\right)^{1/2} \quad (9)$$

Where, G is tension modulus with correct 0 pore fraction. The values of V_l and Vs used to calculate imply wave speed (Vm) which used to calculate Debye temperature turned into calculated using system.

$$\text{Debye temperature} \quad \theta_E = \frac{h}{k}\left[\frac{3\rho q N_A}{4\Pi M}\right]^{1/3} \times V_m \quad (10)$$

Where h, k , M, q and V_m are planks constant, Boltzmann's constant, molecular weight, number of atoms in the unit formula, and means wave velocity respectively.

$$\frac{3}{V_m^3} = \frac{1}{V_l^3} + \frac{2}{V_s^3} \qquad (11)$$

By using relation 8, 9, and 11 values of a longitudinal wave, shearing wave, and mean wave velocity are calculated. Table .3 reflects the longitudinal elastic wave velocity is increased whereas transverse (Shear) wave velocity increased with Ce^{3+} substitution. The wave velocities values of are similar to ferrites value obtained from the UPT method [20]. Table - 3 represents variation of Debye temperature (θ_E) .The Debye temperature expanded with Ce^{3+} substitution. It suggested that lattice vibrations are hindered due to Ce3+substitution. This may be because the electricity of interatomic bonding increases with concentration supported by way of our effects on the version of elastic moduli [19].

The values of V_l/p and V_S/p are calculated through the Anderson equation [21] proven in fig.4.The increases with increasing Ce^{3+} ions substitution. [18].A plot of average sound speed (Vm) against Debye temperature (θE) is shown in Fig.5. It is interesting to word from the discern that the common sound pace increases linearly with the Debye temperature. This behaviour indicates the direct dating among the common sound speed parameter and the critical Debye temperature [22-23].
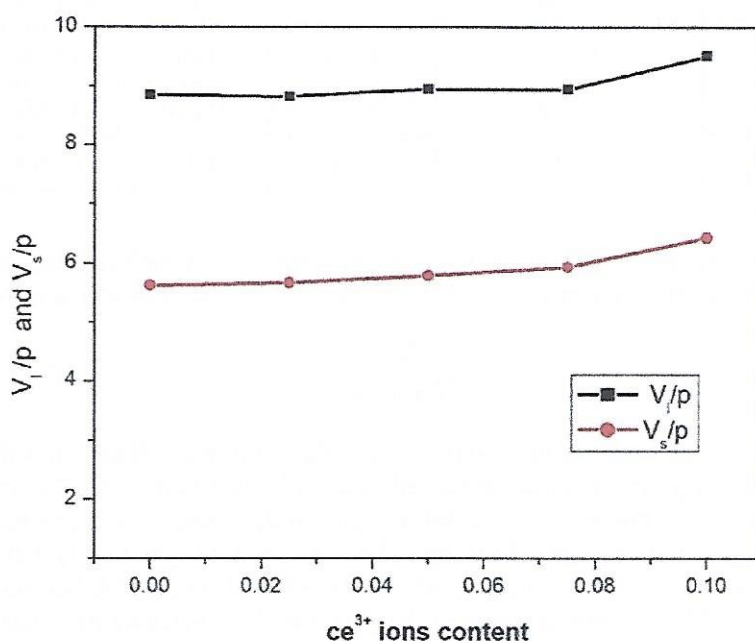

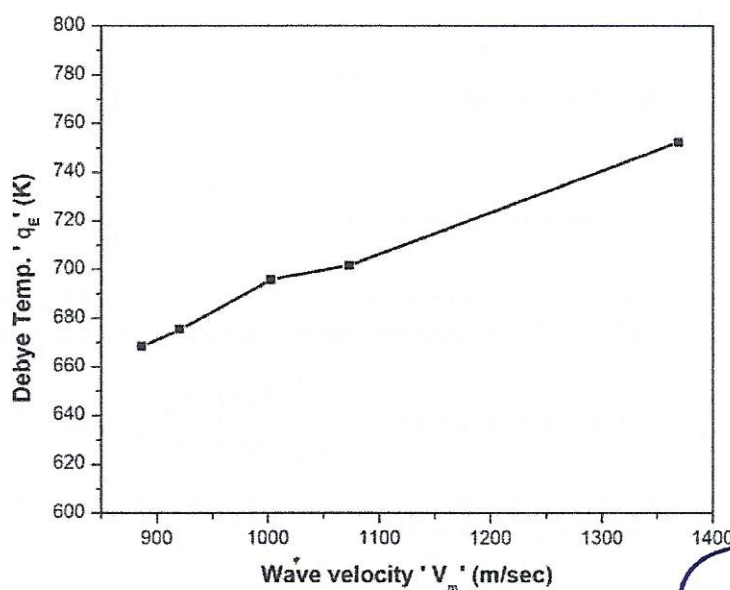**Fig.4: V_l/p and Vs/p in opposition to Ce^{3+} ion content.**

Fig. 5: Debye temperature θ_E in opposition to average sound velocity Vm.

Table No.3. $Cu_{0.5}Zn_{0.5}Ce_xFe_{2-x}O_4$ of (G), (Y), (B), (V_L), (V_S), (V_m) and(Θ_E)areRigiditymodulus,young modulus, Bulk Modulus,longitudinal elastic wave velocity, transverse (Shear) wavevelocity, mean wave velocity,Debye temperaturerespectively.

Comp. x	G	Y	B	V_L	V_S	V_m	Θ_E
0.0	42.29	108.03	80.88	5063.75	3217.84	885.91	668.375
0.025	42.93	109.49	81.23	5078.37	3263.42	920.52	675.348
0.05	45.03	114.73	84.61	5189.47	3360.16	1002.14	695.683
0.075	45.80	116.30	86.13	5192.19	3448.12	1072.80	701.439
0.1	52.73	133.58	95.36	5543.59	3749.15	1369.18	752.291

CONCLUSION

The Ce^{3+} substituted $Cu_{0.5}Zn_{0.5}Ce_xFe_{2-x}O_4$. (x = 0.1,0.075,0.050,0.025,0.0). ferrite nanoparticles have been organized via the usage of the sol-gel auto-combustion approach.The IR spectra confirmed the formation of the spinel shape and gave facts about the distribution of ions between the two sites, tetrahedral (A-site) at (566-627 cm^{-1}) and octahedral (B-web site) at (362-418 cm^{-1}).The elastic constants increased with the increase inCe^{3+} content.The elastic moduli and Debye Temperature are found to increase with increasing cerium.

REFERENCES

1. A.R. Lamani, et al. *Indian Journal of Pure & Applied Physics.*,47, 715- 718 (2009).
2. U .Mazhar, Rana.A. Tahir. *Journal of Magnetism and Magnetic Materials.*, **246** , 110 (2002).
3. A.Y. Lipare, P.N.Vasambekar, A.S. Vaingankar. *Physica Status Solid A.*, **196(2)** , 372–378 (2003).
4. S.M. Patange, S.E.Shirsath, K.S. Lohar, S.G. Algude, S.R.Kamble, N. Kulkarni, K. M. Jadhav. *Journal of Magnetism and Magnetic Materials.* **325**, 107-111 (2013).
5. R.D. Waldron. *Phys. Rev.*99, 1727 (1955).
6. A .Pradeep, G. Chandrasekaran.*Materials Letters.*, **60 (3)** , 371-374 (2006).
7. K.B. Modi, S.J. Shah, N.B. Pujara, T.K. Pathak, N.H. Vasoya, I.G.Jhala. *Journal of Molecular Structure.* **1049**, 250-262 (2013).
8. R. Vishwarup, S.N. Mathad.Materials *Science for Energy Technologies.*,**3** 559–565(2020)
9. V.K. Lakhani, K.B. Modi. *Solid State Sciences.*, **12(12)** , 2134-2143 (2010).
10. V.G. Patil, S.E. Shrisath, S.D. More, S.J. Shukla, K.M. Jadhav. *J. Alloys Compd.*, **488**,199-203 (2009).
11. D. Ravinder, K.V. Kumar, B.S. Boyanov. *Materials Letters.*, **38(1)** , 22-27 (1999).
12. L .Zhang, Y .Wang, B. Liu, J .Wang, G .Han, Y .Zhang. *Ceramics International.*, **47 (8)** , 10927-10939 (2021).
13. G. Allaedini, S.M. Tasirin, P. Aminayi. *International Nano Letters.*, **5 (4)** , 183-186 (2015).
14. T .Tago, T .Hatsuta, K.Miyajima, M . Kishida, S .Tashiro, K .Wakabayashi. *Journal of the American Ceramic Society.*,**85 (9)**, 2188-2194 (2002).
15. N.D.Chaudhari, R.C. Kambale, J.Y. Patil, S.R. Sawant, S.S. Suryavanshi. *Materials Research Bulletin.*, **45 (11)**, 1713-1719 (2010).
16. A .Sutka, G .Mezinskis. *Frontiers of Materials Science.*, **6 (2)** ,128-141 (2012).
17. T.K. Pathak, J.U. Buch, U.N. Trivedi, H.H. Joshi, K. B. Modi. *Journal of nanoscience and nanotechnology.*, **8(8)** , 4181-4187 (2008).
18. S.S. Bhatu, V.K. Lakhani, A.R. Tanna, N.H.Vasoya, J.U. Buch, P.U. Sharma, K. B. Modi. *Ind. J. Pure Appl. Phys.*,**45** ,596(2007).
19. S.A. Mazen, T.A. Elmosalami.*ISRN Condensed Matter Physics.*, **9**,25(2011).
20. Wooster WA. *Reports on Progress in Physics.*,**16 (1)**: 62(1953).
21. O.L.Anderson. New York USA: Academic Press,(1965).
22. P.V. Reddy. *Physica Status Solidi A.*, **108 (2)** , 607– 611 (1988).
23. Revathi MB, Rao TS. *Journal of the Less-Common Metals.*,**34 (1)**, 91-96 (1974).

Principal

Jawahar Arts, Science & Commerce College, Andur Tal. Tuljapur Dist, Osmanabad